Defects and spatiotemporal disorder in a pattern of falling liquid columns

Philippe Brunet* and Laurent Limat†

Laboratoire de Physique et Mécanique des Milieux Hétérogènes UMR 7636 CNRS - Ecole Supérieure de Physique et Chimie Industrielles 10, rue Vauquelin, 75231 Paris Cedex 05, France

(Received 27 February 2004; revised manuscript received 2 June 2004; published 20 October 2004)

Disordered regimes of a one-dimensional pattern of liquid columns hanging below an overflowing circular dish are investigated experimentally. The interaction of two basic dynamical modes (oscillations and drift) combined with the occurrence of defects (birth of new columns, disappearances by coalescences of two columns) leads to spatiotemporal chaos. When the flow rate is progressively increased, a continuous transition between transient and permanent chaos is pointed into evidence. We introduce the rate of defects as the sole relevant quantity to quantify this "turbulence" without ambiguity. Statistics on both transient and endlessly chaotic regimes enable to define a critical flow rate around which exponents are extracted. Comparisons are drawn with other interfacial pattern-forming systems, where transition towards chaos follows similar steps. Qualitatively, careful examinations of the global dynamics show that the contamination processes are nonlocal and involve the propagation of blocks of elementary laminar states (such as propagative domains or local oscillations), emitted near the defects, which turn out to be essential ingredients of this self-sustained disorder.

DOI: 10.1103/PhysRevE.70.046207 PACS number(s): 05.45.−a, 47.54.+r, 82.40.Bj

I. INTRODUCTION

In the last two decades, considerable effort has been devoted to the understanding of how complexity and unpredictability arise in spatially extended systems. For this purpose, studies of one-dimensional pattern-forming instabilities are particularly instructive [1,2]: in such systems, the one-dimensional nature enables a simple visualization of the dynamics by spatiotemporal diagrams, and the different steps which drive the dynamics towards disordered states can be clearly identified. These steps generally involve the loss of certain space-time symmetries underlying the basic static pattern [3]. Moreover, spatiotemporal chaos (STC) occurring in such systems is supposed to have some qualitative similarities with weak-developed turbulence in fluids [4,5].

The most famous of these pattern-forming systems are probably the Rayleigh-Bénard (buoyancy) and the Bénard-Marangoni (thermocapillary) convective instabilities [6–8]. Other quantitative studies have been performed on centrifugal convective instabilities, namely, Taylor-Dean [9] and Taylor-Couette flows [10]. A specific class is composed of instabilities involving the destabilization of an interface: directional viscous fingering [11–13], directional solidification [1,14,15], and liquid column arrays formed by a Rayleigh-Taylor instability below a 1D circular ceiling [16–19]. More "exotic" systems were imagined, still involving an interface, such as, for instance, a liquid ridge inside an horizontal rotating cylinder [20,21] or a circular array of ferrofluid pikes induced by a normal magnetic field [22].

This enumeration is far from exhaustive (for more complete references, see the bibliography of Refs. [2,23]), and lots of these experiments evidenced a transition to spatiotemporal chaos via "spatiotemporal intermittency" (STI), similar to what is observed in weakly turbulent flows: a coexistence of laminar and turbulent domains, separated by fronts fluctuating erratically in time and space. In the present paper, we focus our attention to the circular array of liquid columns [16–19]: a viscous liquid overflows from a circular dish fed at constant flow rate, the resulting pattern being reproduced in Figs. 1(a) and 1(b). In this system; disorder appears with a scenario seemingly different than STI.

Basically, this experiment combines a Rayleigh-Taylor (RT) instability of the liquid hanging below the dish and a constant supply of liquid (at flow rate per unit length Γ). Usually, the RT instability, resulting because of the combined actions of destabilizing gravity and stabilizing surface tension, tends to create a pattern of pendant liquid drops, with a typical spacing $\lambda_{RT}=2\pi\sqrt{2}l_c$ **(**$l_c=[\sigma/(\rho g)]$ being the capillary length defined upon surface tension σ, mass density ρ, and gravity g**)**. The addition of a constant supply (with a minimal Γ of 0.05 cm^2/s) turns this pattern into a periodic array of columns with a spacing slightly smaller than λ_{RT}. Contrary to the pendant drops, the array of columns exhibits collective behaviors, accompanied by wavelength modulation: depending on the relative motions of neighboring columns, the local wavelength can vary from 0.8 to 1.9 times the RT theoretical wavelength [see Fig. 1(c)].

Our previous investigations have evidenced that it behaves in a way very similar to directional viscous fingering or directional solidification: spatially extended oscillations, each column oscillating while remaining out of phase with its neighbors, drift at a constant speed of "tilted" domains in which the left-right symmetry is broken, coalescence and nucleation of cells, etc. Therefore, its study is of great interest for extracting general features concerning the dynamics of this specific kind of interfacial system.

*Present adress: Department of Mechanics - Kungliga Tekniska Hogskolan, 10044 Stockholm, Sweden. Electronic address: brunet@mech.kth.se; URL: http://www.pmmh.espci.fr/~brunet

†Also at: Fédération de Recherche Matière et Systèmes Complexes, FR 2438 CNRS, France. Electronic address: limat@pmmh.espci.fr

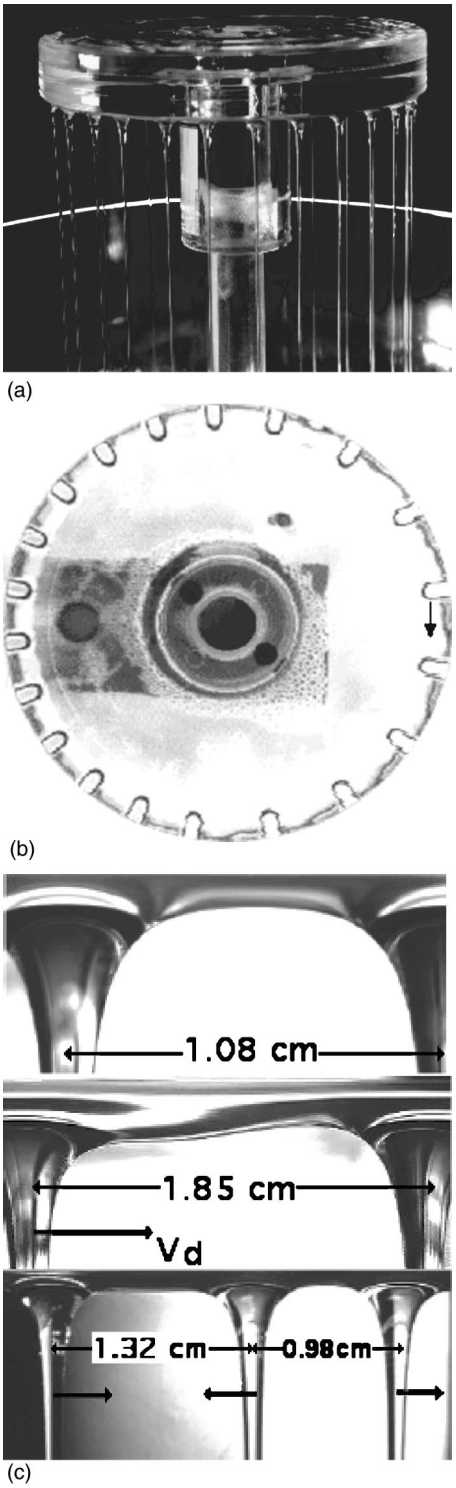

FIG. 1. The circular fountain experiment. (a) A side view of the array of liquid columns (dish radius R_e=5 cm, silicon oil 100 cP). (b) The array viewed from above. (c) Magnified views of arches connecting two columns. From top to bottom, static columns (homogeneous and reduced spacing, symmetrical shape), drifting columns (homogeneous dilated spacing, asymmetrical arch), and oscillating columns (alternatively dilated and shrunk spacing, symmetrical arch).

Moreover, this system offers several advantages for an exhaustive quantitative study of spatiotemporal chaos: (1) the scenario of successive secondary bifurcations summarized above is rather simple, and combinations of these instabilities lead to chaotic spatiotemporal diagrams of "good" quality (i.e., the columns trajectories in spatiotemporal diagrams remain always very well defined, without any local disappearance of the pattern). (2) The circular geometry provides periodic boundary conditions which prevent any perturbations from edges. Even if the system has a finite size, it enables propagative domains — having an essential role in chaotic regimes as we shall see — to evolve as if they were in an infinite medium. (3) As explained in our previous papers [16–19], one can control initial conditions (number of columns and their positions) very easily by playing with a needle put in capillary contact with the columns.

These properties introduce the pattern of liquid columns as a convenient workbench to study spatiotemporal chaos in the general dynamics of fluid fronts. The study of this system, related in the present article is focused towards two questions. (1) Qualitatively, how does disorder arises after successive bifurcations and progressive losses of space-time symmetries? (2) What are the statistical properties of chaotic regimes? To answer this second point, it is necessary to define relevant quantities to be measured in our system, which are not so obvious at first sight. To justify the use of a particular framework, it is now important to quote some previous endeavors in others experiments or numerical models.

A. Historical context

Contrary to geometrically confined systems, in which chaos has only a temporal signification, chaos in spatially extended systems can involve both a loss of time and space coherence. Despite numerous studies, classification of extended systems with universal criterions is still a subject of debate [24]. Such systems are not easily reducible into a set of minimal generic equations, and it is most often impossible to achieve a direct resolution at a "microscopic" level. That is the reason why it is often necessary to borrow methods from statistical physics or out-of-equilibrium thermodynamics. Among various attempts, a conjecture by Pomeau [25] drew similarities between STI and stochastic models of directed percolation (DP). In both situations, disorder spreads by contamination processes.

Few years later, Chaté and Manneville studied the statistical properties of numerical deterministic systems such as time-iterated coupled map lattices (CML's), the complex Ginzburg-Landau equation (CGLE) or the damped Kuramoto-Sivashinsky equation (DKS) [26], which reproduce the qualitative behaviors of many experimental systems. One of the aims of these studies was to put into evidence that, in such deterministic models, disorder spreads by contamination in a similar way to the DP. Measurements have been focused on critical exponents, deduced from divergence laws for characteristic lengths and times. It turned out that systems exhibiting STI (the numerical models mentioned above and a host of others systems) do not make up a universal class: there exist almost as many set of exponents

as studied systems [22]. Very few of them have critical exponents close to the ones measured or calculated in DP. However, these studies provided some hints to relate exponents values and mechanisms involved in disorder: recent studies in deterministic numerical models have shown that the occurrence of long-lasting solitonlike structures could change the universality class [27] and even the order [28,29] of the transition to chaos via STI. These studies have pointed out the role of propagative structures — which can generate turbulent sites in their wakes or by colliding each others — in the breakdown of universality with stochastic models. Otherwise, discontinuous cases of CML's have been thus successfully used to mimic the transition to turbulence in a plane Couette flow [30], where the transition to STI is a first-order one (discontinuous).

Until now, measurements of the critical exponents is one of the sole methods to classify chaos in extended systems. In many experiments, transition toward disorder (via STI or not) is continuous so that critical exponents exist and can be measured. Statistical studies on pattern-forming instabilities were first achieved in the RB convection [7,8], where divergences of length and time correlations where measured. Similar behaviors were found in disordered cellular interfacial fronts, such as in the printer's experiment [12], in the Taylor-Dean system [9], in the Taylor-Couette experiment [10], or more recently in a system of ferrofluid pikes under oscillating magnetic field [22]. In this last experiment, the authors found that most of the critical behaviors could be correctly fitted by exponents of stochastic models. They concluded that the ability of disordered states to appear spontaneously within pure laminar domains (i.e., the absence of a real "absorbing state" in experiments) could explain the discrepancy with critical properties of stochastic models. Indeed in most experimental systems, laminar domains (characterized by predictable dynamics inside them) include a host of states which can behave differently in regards to disorder [31]. In the same manner as iteration laws of coupled maps can dramatically influence the transition, the successive bifurcations leading to chaos could also be determinant factors in cellular patterns. That is also why disordered states occurring in such patterns, despite finite-size limitations [32], are of great interest as an alternative way of numerical studies.

Otherwise, there often exist striking similarities between numerical models mentioned above and experiments, and models are not only studied for their own properties but also to mimic realistic systems. For example, the DKS equation [33,34] has appeared relevant to describe the dynamics of growing interfaces. A study of this equation in a confined geometry showed similarities with the dynamics of some solidification fronts, supported by the fact that the DKS equation can be obtained from general considerations about mechanisms governing the dynamics of an interface [35]. However, a recent study showed that the transition toward chaos (via STI) in DKSE was discontinuous [4,36], although in most pattern-forming unstable fronts, the transition turned out to be continuous.

B. Liquid column array: a brief survey

As we shall see, the pattern of columns introduced above seemingly shows a continuous transition to disorder after successive bifurcations, so that it is tempting to study it in the usual framework presented before: the seek for critical behaviors. It had been emphasized in previous studies [17,19] that disorder should be the result of interactions between coexisting dynamical regimes (propagative domains, oscillations, etc.). This is evidenced by the diagram on Fig. 2. Considered on their own, these laminar regimes are stable within various ranges of the natural control parameter: the flow-rate per unit length Γ (flow rate divided by the perimeter of the array). Moreover, they appear in a specific range of local wavelength. Starting from a static state and increasing flow rate can lead to oscillations of columns in phase opposition. Occurrences of dynamical regimes can also be related to modifications in the number of columns. A crucial example is the following: by decreasing the number of columns, one can initiate motions of several consecutive columns, which create a stable propagating domain of drifting columns, with dilated spacing between them (see the experimental method in Refs. [16,17]). One visualizes the dynamics of the pattern by means of spatiotemporal diagrams: three of them are shown in Figs. 3(a)–3(c), showing, respectively, a propagative domain of drifting columns (followed by transient oscillations), an extended oscillating regime, and a global regime of drifting columns. The period of oscillations is a reliable measurement of a characteristic time in the system. This duration was found to decrease with flow rate [18,19] and varies around one second.

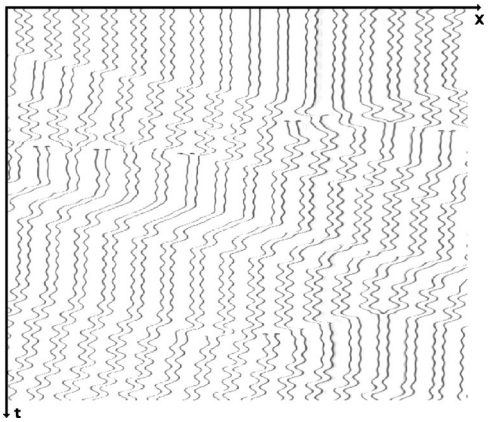

FIG. 2. Extract from a diagram of spatiotemporal chaos. Disorder is sustained by nontrivial combinations between basic dynamical regimes (oscillations and drifts). $\Gamma = 0.420$ cm^2/s.

In previous studies, it has been observed that local spacing between columns is related to their dynamical behavior: if the pattern is locally shrunk (i.e., columns are distant from one another by 0.9 to 1.1 cm close to the most unstable Rayleigh-Taylor wavelength), columns remain static. If it is locally dilated (from 1.5 to 2.1 cm), columns drift as a consequence of the growth of an antisymmetric mode which breaks the left/right symmetry of arches linking two columns [see Fig. 1(c)] A stability diagram (Fig. 4) is presented to clarify the relative locations of dynamical regimes in the space of control parameters. It is plotted upon mean wavelength λ_M (inversely proportional to the number of columns N) and flow-rate per unit length Γ. SC, OSC, LD, and GD, respectively, stand for static columns, oscillations, local

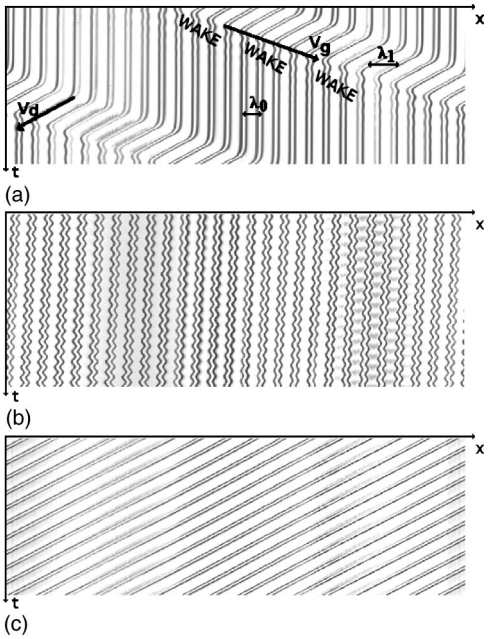

FIG. 3. Spatiotemporal diagrams of basic states. Time runs vertically, from top to bottom. The horizontal axis is the position of columns along the dish (here radius R_e=5 cm). (a) A localized domain of drifting columns. One can measure the velocity of the domain walls (v_g), of the drifting columns (v_d), the wavelength inside the domain (λ_1), and selected outside (λ_0), where an oscillating wake can appear (Γ=0.232 cm^2/s). (b) Oscillations of columns out-of-phase with nearest neighbors (Γ=0.310 cm^2/s). (c) A state of (global) drifting columns extended to the whole perimeter (Γ=0.274 cm^2/s).

drifts, and global drifts. The smaller the number of columns is, the fewer the share of static columns. Hatched areas stand for ranges of parameters that are impossible to reach. This diagram also includes a large domain of spatiotemporal chaos (STC), for higher flow rates. This last area defines the range of parameters for which the system is permanently in a

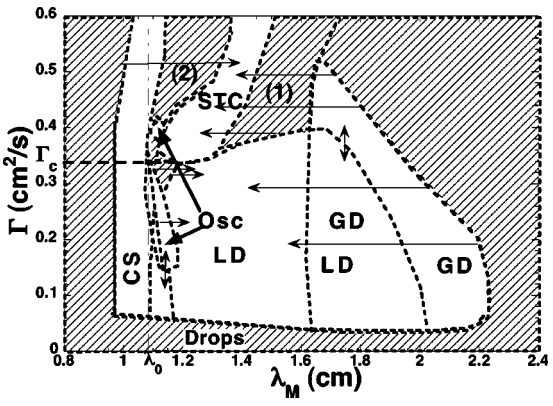

FIG. 4. Stability diagram in the space of control parameters: mean wavelength λ_{moy} and flow-rate per unit length Γ. The threshold Γ_c is the highest value of flow-rate above which an ordered regime breaks up, and becomes a chaotic one; arrows illustrate some possible evolutions from a regime to another one (see Sec. III for further explanations).

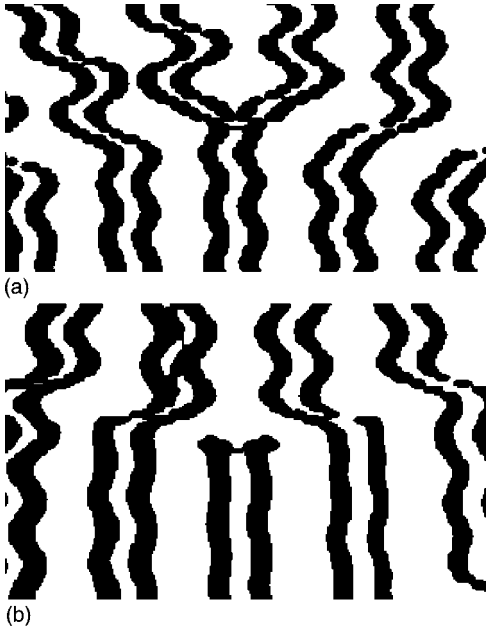

FIG. 5. Magnified views on spatiotemporal diagrams enlightening the two kind of defects leading to chaotic dynamics. (a) The fusion of two columns into one single. (b) The birth of a column between two neighboring ones.

chaotic state, and where N fluctuates and cannot be controlled any longer. Elsewhere, chaotic regimes can appear but only transiently: the system will then be attracted towards one of the laminar regimes cited above. The reached laminar regime will depend on initial conditions, but not through a trivial relation. In both transient and permanent cases, chaos is associated to fluctuations in the number of columns. In the array of liquid columns, any change in the number of columns is called a "defect," so that it can correspond to two kinds of events: the fusion of two columns into a single one (−1) or the birth of one new column between two neighboring columns (+1) (see extracts in Fig. 5).

Finally, it is worth mentioning a particular regime which is composed of small consecutive propagative domains. This is not obtained by the will of the experimentalist, but rather spontaneously after long chaotic transients. An example is shown in Fig. 6. This state has the remarkable property to exhibit a spatial "triperiodicity," i.e., the motions of columns are identical each third column.

The aim of this paper is to present a statistical study of chaotic regimes in the circular array of liquid columns on both transient and permanent situations. To fulfill this purpose, it has been necessary to define a criterion to measure the turbulence that is relevant for our system, as will be seen in Sec. III. In addition, this paper focuses on others questions. Can one measure any critical behavior in this system? If transition to chaos does not proceed via STI, does disorder behave as a contaminating process anyway? This last point cannot be answered with just a few words. One first has to carefully identify the mechanisms which create disorder in our system. An entire section (VI) in this article is dedicated to it.

The paper is organized as follows. In Sec. II the experimental setup is described. In Sec. III, we first expose general

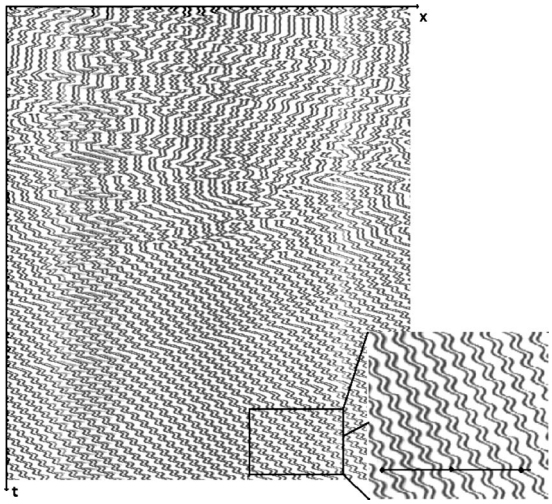

FIG. 6. Convergence of an initially chaotic state towards a particular state mixing oscillations and drift, with a spatial period three times larger than the mean spacing between columns (see inset). $\Gamma=0.26$ cm^2/s, $\eta=200$ cP. The total duration is around 80 s.

features of chaotic regimes in our system. This is followed by arguments, based on experimental observations, that have led us to the choice of the defect rate (number of defects per unit time) to quantify turbulence. In Sec. IV the study of transient chaotic states is presented, followed by the study of "stable" chaos (Sec. V). Section VI focuses on the mechanisms creating disorder, towards the links between defects and local occurrences of deterministic regimes.

II. EXPERIMENTAL SETUP

Silicon oil of viscosity $\eta=100$ cP, surface tension $\sigma=20.4$ dynes/cm, and density $\rho=0.97$ g/cm^3 at 20 °C is injected at the dish center through a hollow vertical tube. The flow is measured by a float flow meter (Brooks full view GT 1024) and kept constant by a gear pump (Ismatec BVP Z) followed by a cylindrical damping chamber (half filled) (radius=20 cm, height=15 cm). The imposed flow-rate Q ranges from 2 to 30 cm^3/s. The oil temperature is regulated with a thermal bath at 20 °C with a few percent accuracy. Plexiglas circular dishes with different external radius (R_e) have been used. One defines the flow-rate per unit length $\Gamma=Q/2\pi R_e$, which appears to be the relevant control parameter. It can be determined with an accuracy of ± 0.005 cm^2/s. The data reported here were obtained with two dishes of radii $R_e=5$ cm and 8.35 cm. The accuracy of the dish horizontality is crucial for a quantitative study. It is tuned with a three-foot table supporting the setup, by simply checking the uniformity of oscillation amplitudes of columns when the system undergoes a transition to an oscillatory state [Fig. 3(b)].

Observed from above by a CCD video camera, and lit by a circular neon tube put in the periphery of the dish and slightly below it, the pattern appears as a series of U spots [see Fig. 1(b)]. Spatiotemporal diagrams are built by recording grey levels along the circle on which the column centers are moving. Experimentally, the radius of this circle was

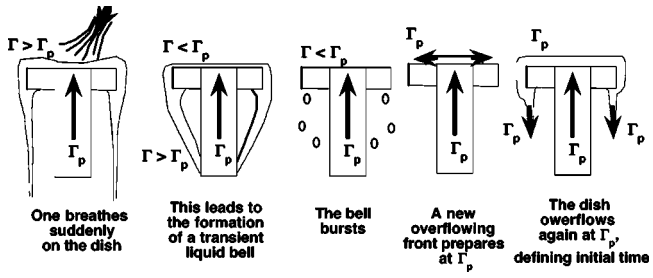

FIG. 7. Diagram describing the initialization of the system. Γ_p is the flow rate imposed by the pump.

found to be independent on the flow rate [16,17] and, respectively, equal to $R=4.77$ cm and $R=8.10$ cm for the dishes of radius $R_e=5$ cm and $R_e=8.35$ cm. Images were digitized using NIH Image 1.62 on a Macintosh computer. To achieve reliable image processing, it is important that the background color of pictures acquired from above would be as homogeneous as possible and that the edge of columns would be visibly sharp, in order to have well-controlled diagrams; Several pieces of black papers cover the surround between the dish and the neon tube to prevent unwanted light reflections.

Special care is also devoted to protect the system from any source of perturbation. The dish is surrounded by a transparent plexiglas cylinder of internal diameter $d=18$ cm, to protect the system against any air motions around the experiment. Moreover, in order to isolate the dish from vibrations induced by the thermostatic bath or the gearing pump, these devices are put on foam beds of a few centimeters height each.

The viscosity of 100 cP has been chosen to constitute a good compromise between two conditions, based on the following observations. Chaos is not observed for lower viscosities, as was revealed by some attempts with several viscosities from 10 to 70 cP. At higher viscosities, the transition to chaos seems somehow perturbed by the omnipresence of the triperiodical state described above, which complicates the stability diagram. In a large range of flow rate, this state is the only stable attractor and competes with the chaotic regime. Thus, critical properties which are of interest here appear more clearly with the 100 cP oil, where this state is stable in a much smaller range of parameters.

In most measurements reported in this article, it has been necessary to "initialize" the pattern of columns, which means to obtain a new set of initial conditions from which the pattern evolves at fixed flow rate. To achieve practically this goal, the best procedure is to suddenly cut off the flow of liquid, and to sharply restart it. To generate this step of flow rate, one proceeds as illustrated in Fig. 7. An important question is how broad the range of possible initial conditions is. From careful examinations of spatiotemporal diagrams, it turned out that this process first creates initial conditions which are close to one another. When the liquid starts to overflow again, it creates an homogeneous pattern of wavelength around 1.30 cm. However, this state is very unstable and during the first second, many defects appear [see Figs. 8(a) and 8(b)]. As a consequence, the system behaves in a

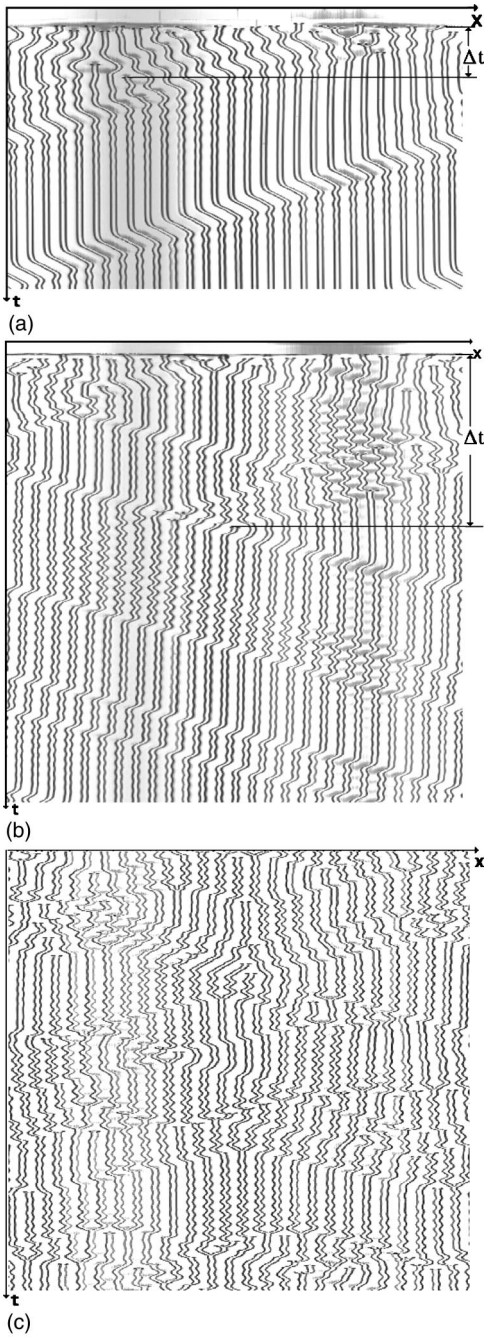

FIG. 8. Examples of disordered dynamics in the pattern of columns. (a) At a flow rate (0.14 cm^2/s) smaller than the threshold Γ_c, the pattern reaches predictable, periodic dynamics after a chaotic transient. ΔT (here 3.5 s) corresponds to the duration between the initialization of the system and the occurrence of the last defect. (b) Same as (a) but at larger flow rate (0.28 cm^2/s): the duration Δt (here 13.4 s) of the chaotic transient is larger. (c) For flow-rates above threshold Γ_c (here, $\Gamma=0.46$ cm^2/s), the pattern is endlessly chaotic.

very chaotic way and is rapidly uncorrelated from the initial state. In others words, after only one second, each "initial condition" has been driven towards a state very different from one another.

III. QUESTIONS TO TACKLE PRIOR TO THE STUDY OF CHAOTIC REGIMES

The study of critical behaviors suggested in the historical background needs a well-defined threshold. It has been mentioned that chaos could occur both transiently or permanently, so that we expect to find remarkable properties at the transition (in the following, the adjective "permanent" is omitted, considering that chaos is permanent if no further detail is mentioned). Referring to the stability diagram, one defines Γ_c as the minimum flow rate which belongs to the curve separating the STC domain and domains of laminar regimes (see Fig. 4). Below this threshold, it is observed that the system *always* catches a laminar state after a chaotic transient. However, as reported on the stability diagram, there exist stable laminar states for $\Gamma > \Gamma_c$, for extreme values of λ_M: these states are either composed by a global drift, by extended localized domains, or by shrunk static states. During the numerous runs of the system, these conditions have never been reached spontaneously from a chaotic state. In others words, these states thus require specific initial conditions that only the experimentalist is able to provide. The hatched areas between STC and these states [labeled (1) and (2) in the diagram], can only be crossed through one way, from order to chaos. To summarize, conforming to the features of our system emphasized above, the following definition is chosen: the threshold Γ_c from order to disorder is defined as the value of the flow rate above which the pattern will stay chaotic and will not catch a laminar attractor.

One question still remains to achieve a study of disordered regimes: how to quantify disorder in our system? The quantification of turbulence is generally obvious in numerical systems. In coupled map lattices, for example, a site is defined as turbulent if the function associated to this site has a value included in a fixed "turbulent interval" (corresponding to an area where no fixed point lies for the basic function). In studies of the KSA equation, a site is considered as turbulent if the peak-to-peak amplitude is lower than a given threshold [26]. In experimental systems, this amplitude — similar to the "height" of a cell — is generally more difficult to measure. In most pattern-forming experiments, the pattern is considered as locally turbulent if the wavelength gradient or the temporal variations of the wavelength are large enough [8,22]. In the array of liquid columns, such a criterion is not relevant. Indeed, there exists dynamical states combining large local variations in the spacing between columns and completely predictable dynamics (for example, local [Fig. 3(a)] or global drifting [Fig. 3(c)] and triperiodic (Fig. 6) states). Criteria of turbulence deduced from the wavelength gradient also do not fit with our system because the triperiodic ("oscillating-propagating") state (Fig. 6), which is perfectly predictable, has locally large wavelength gradients. If we consider temporal variations of the wavelength, they can be locally large near defects as well as in predictable oscillations, so that no criterion for turbulence can be built upon this quantity. Finally, another possible criterion built on the absolute value of the wavelength is also put into fault. Indeed, the global drifting state [Fig. 3(c)] can have local spacing between columns larger than what is needed to enter a chaotic regime: parity-broken cells can

hold a much larger wavelength than symmetrical ones without breaking. Thus, usual criteria differentiating laminar and turbulent states in pattern-forming instabilities cannot be applied in our system.

The only topological criterion of chaotic dynamics is the presence of defects, i.e., a nonconstant number of cells. In others words, the presence of these defects is a necessary and sufficient condition to have unpredictable behavior, that is, at least it is what our long and numerous acquisitions led us to conclude. It is thus natural to choose the rate of defects (number of defects per unit time) as a relevant quantity to measure chaos in our system. In fact, these considerations reveal a major characteristic of the pattern of columns. In most of the studies of STC indeed, disorder is quantified by the "turbulent fraction," i.e., the mean surface filled by turbulent domains in the (x,t) plane. As no geometrical criterion holds to define turbulent or laminar areas in our pattern, there is not any binary structure sharing it between laminar or turbulent domains. Consequently, one cannot access the length and time distributions of laminar/turbulent regimes. In other systems these distributions, deduced from the binary structure in spatiotemporal diagrams, could lead to the measurement of two critical exponents. The concept of a turbulent behavior involving topological defects was first introduced by Coullet and co-workers [38] in the 2D model equation of Ginzburg and Landau. The denomination of "defect-mediated turbulence" (DMT) was defined and the authors put in evidence a discontinuous transition from a plane-wave state to this regime (a jump to a nonzero value of defect rate exists just above the threshold). Several systems have shown DMT, although most of these are two-dimensional ones: for example, convection induced by an electric field [39], model equations of excitable media [40], and more recently inclined layer convection [41]. A study on model equations of convection pointed out that defects appear inside areas where Lyapunov exponents are larger than zero (i.e., responsible for sensitivity to initial conditions) [42]. The obvious link between presence of defects and unpredictable dynamics in our system can be put in relation with this assertion. Also in the complex Ginzburg-Landau equation model, chaotic sequences can include a defect-phase regime where defects, which are singularities in the spatial phase, play a role of self-sustaining disorder (see, for example, Ref. [43]). However, we only mention here a possible nature for chaos in our system: the present study does not really answer if DMT occurs here.

In our experiment, defects are counted as follows. We have programmed a "macro" in the software NIH IMAGE, which extracts the number of columns after a grey level threshold procedure. The number of columns is acquired 25 times per second. The time step of $1/25$ s is much smaller than the characteristic time of the system (approximately 2s). Defects are then calculated by the absolute difference of two consecutive numbers of columns. The consequence is that simultaneous creation and annihilation $(+1-1=0)$ at the same time step should not be taken into account in the counting. Nevertheless, careful inspections of spatiotemporal diagrams have shown that such events are rare, and may play a significant role only in extreme situations: in chaotic states very far from threshold Γ_c (where the number of defects per second can exceed 10) or during the first second of chaotic transients, where defects are generally numerous (but which are not taken into account in the measurements of critical exponents, as mentioned later).

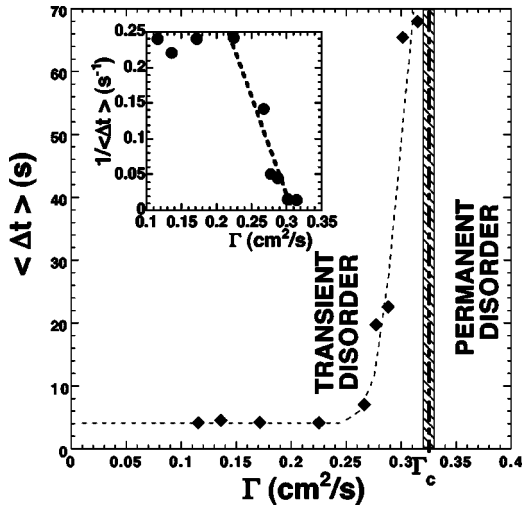

FIG. 9. Mean duration of chaotic transients versus flow rate. The dashed curve is a guide for the eye. $\eta=100$ cP. The inset shows that Δt is correctly fitted by a law $(\Gamma_c-\Gamma)^{-1}$, although the range of exponent values is broader.

Quantitative measurements have been considered in two different points of view depending on whether flow rate is below or above threshold Γ_c. Several critical exponents are deduced from statistical behaviors of chaotic transients, for which investigation methods are quite different than usual: instead of making statistics on long acquisitions of chaotic states, one has to extract mean behaviors from many acquisitions with different initial conditions. This unusual approach was already carried out in the plane Couette experiment (discontinuous transition), comparatively to coupled-map lattices [30], but to our knowledge this is the first time that critical exponents will be deduced from chaotic transients in an experimental system.

IV. STATISTICAL STUDY ON CHAOTIC TRANSIENTS

If $\Gamma<\Gamma_c$, defects are counted during chaotic transients. A step of flow rate is first created by the previously described method (Fig. 7). The initial time is fixed when the liquid overflows again from the dish (evaluated with a precision of ± 0.1 s). Acquisitions are stopped when the pattern seems stable enough to stay in the current state, i.e., that the number of columns remains constant. This criterion is appreciated *de visu* by a direct observation of the motions of columns. For a given value of the control parameter, the flow rate Γ, 250 acquisitions are done, each after an initialization of the system.

Prior to results concerning the counting of defects, we present measurements of mean durations of chaotic transients, i.e., the mean time difference between "initialization" of the system and the occurrence of the last defect. After this last defect, the dynamics is predictable. The final reached state can be static, oscillatory, or can include several propa-

gative domains. In Fig. 9, the mean duration $\langle \Delta t \rangle$ of chaotic transients versus flow rate is plotted. It is shown that the mean duration of transients diverges, approaching threshold Γ_c. At low flow rates, $\langle \Delta t \rangle$ is independent upon flow rate, and increases until Γ_c. The threshold value is

$$\Gamma_c = 0.325 \pm 0.005 \text{ cm}^2/\text{s}. \quad (1)$$

This value is determined by two ways. The first method consists in starting from a high flow rate (typically 0.36 cm^2/s) above the presumed value of Γ_c, and in decreasing it by very small successive steps (0.005 cm^2/s). After each step, one waits for around thirty minutes, which is much longer than the largest mean duration measured below threshold (and even longer than the longest duration measured for a transient), until a stable laminar state is reached. A particular care is devoted to the reliability of this stability. A laminar state is then obtained between 0.32 and 0.33 cm^2/s. Even if we cannot exclude a slight discontinuity or finite-size effects, the error of ± 0.005 cm^2/s is of same order than the error in the flow-meter calibration (this error is due to the direct lecture of the floater position and to the possible power fluctuations of the pump). It is worth mentioning that the same procedure has been done with a larger dish (radius $d=8.35$ cm) and that the same value of flow-rate threshold (per unit length) has been found. This suggests that, even if finite-size effects exist in our system, they do not affect Γ_c.

The second method proceeds with the same logic, except that one starts below threshold (from 0.290 cm^2/s). One increases the flow rate by successive steps of 0.005 cm^2/s. After each step, if the laminar state breaks, one waits for the system to retrieve another laminar regime, and then makes a new decreasing step. If after a duration of thirty minutes the pattern is still chaotic, this means that the threshold has just been overcome. A value around 0.325 cm^2/s is found, similar to those given by the first method. Here also, the same value of Γ_c is found for a larger dish.

The fit of our measurements of mean durations near threshold, by the following power law, determine a first critical exponent

$$\langle \Delta t \rangle \sim (\Gamma - \Gamma_c)^{-\gamma}. \quad (2)$$

This critical behavior denotes a divergence of a characteristic time of the system, near threshold. Varying Γ_c from 0.32 to 0.33 cm^2/s, the agreement is correct but the exponent γ depends on the chosen value for Γ_c. The exponent γ in Eq. (2) can then vary from 0.5 to 1.1. Due to uncertainty on Γ_c and difficulties to run much more measurements near threshold, γ is determined with the following range of error:

$$\gamma = 0.8 \pm 0.25. \quad (3)$$

Of course, these considerations are done under the assumption of a continuous transition, for which characteristic quantities follow power laws near threshold. This has to be admitted at the present stage, even if one cannot exclude that $\langle \Delta t \rangle$ keeps a finite value at threshold. However, the similar values for Γ_c found by the two methods, approaching Γ_c either by minor or major values, is consistent with a unique

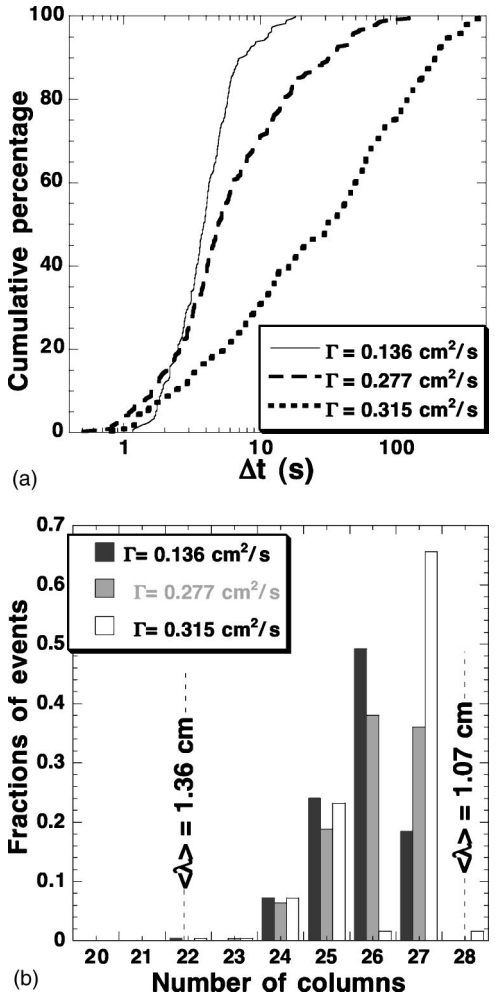

FIG. 10. (a) Number of transients of duration smaller than $\langle \Delta t \rangle$ presented as a cumulative percentage (over 250 acquisitions), for three flow-rate values. The case $\Gamma = 0.315$ cm^2/s is close to threshold. (b) Histograms of numbers of columns (and corresponding mean wavelength) of laminar states obtained after chaotic transients, for three different flow rates (250 acquisitions). Dish radius $R_e = 5$ cm for (a) and (b).

threshold, and so on with a continuous transition. In systems exhibiting a continuous transition to chaos via STI, an exponent can be deduced from distributions of laminar domains lifetimes just above threshold (noted ν_t in most studies). In our system, the exponent γ could be the equivalent of ν_t [37], although measured just below threshold. Indeed, in several experiments [22], a value for ν_t close to ours is found. Beyond the determination of a critical exponent, a detailed look at the distributions of durations is instructive. These distributions are reported in Fig. 10(a), as a cumulative percentage of number of events of duration smaller than the variable Δt. As noticed above at the end of Sec. II (but without any empirical proof), the system evolves through very different ways during the first second after initial time, despite initial stages are similar to each others for most of the acquisitions. The huge dispersion of values for Δt evidences the high sensitivity to initial conditions.

Another point to mention is that the duration of a chaotic transient does not seem to be linked with the final laminar

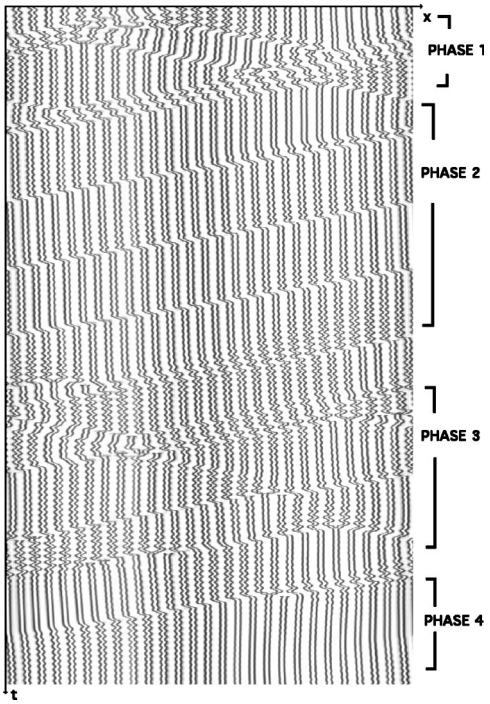

FIG. 11. Example of convergence towards a laminar state, just below threshold. During phase 1, the pattern is disordered, until it reaches a laminar state (phase 2). But this state is unstable and the pattern enters again a chaotic regime (phase 3), and finally converges to a stable laminar state (phase 4). The total duration is 68 $\Gamma = 0.30$ cm^2/s.

state, for a given flow rate. If one tries to build statistics on final states, it appears that the only reliable quantity to compare, is the number of columns. Figure 10(b) represents histograms of events corresponding to several possible numbers of columns in the final state. At small flow rates, the dominant reached state contains a propagative domain the size of which is minimal (corresponding to $N=26$ columns, with a dish radius of 10 cm), see Fig. 8(a). At higher flow rates, near threshold, the dominant state is the extended oscillating regime (27 columns) [Fig. 3(b)], since a single small propagative domain appears more and more unstable. A typical example is shown in Fig. 11: after a chaotic transient (phase 1), the system first catches a 26-columns state (phase 2), but this state is unstable and breaks to enter again a transient chaotic regime (phase 3), and to finally reach a stable oscillating regime (27 colums, phase 4). This example illustrates how the progressive loss of stability for basic laminar states, at increasing flow rate, may cause an increase of the mean duration $\langle \Delta t \rangle$. The system has to "explore" more and more configurations until it reaches a stable one.

In addition to statistics on final states, it is of interest to scan how disorder evolves during transients. Figure 12 shows the total sum of defects versus time, during each time step of the 250 acquisitions, for a flow rate of $\Gamma = 0.315$ cm^2/s (just below Γ_c). The decrease of defect occurrences is due, on one hand, to the broad distribution of transient durations and, on the other hand, to the decrease of the rate of defects with time during a single acquisition. For a sufficiently large number of acquisitions, Fig. 12 could illus-

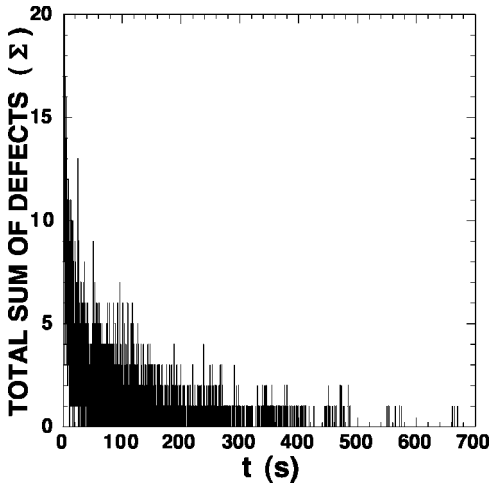

FIG. 12. Total sum of defects during the 250 acquisitions, just below threshold ($\Gamma = 0.315$ cm^2/s).

trate the probability to encounter a defect at time t after initialization. However, this total sum shows sharp variations versus time, so that a quantitative study requires one to define and plot another quantity: the defect rate, i.e., the number of defects per unit time, for a duration larger than a time step. This quantity, which evolves smoother with time, can be more conveniently fitted by an analytic expression.

For each acquisition, the defect-rate is defined as

$$\rho = \frac{D(t+\delta t, t)}{\delta t}. \tag{4}$$

$D(t+\delta t, t)$ is the number of defects during the time interval $[t, t+\delta t]$. δt is chosen to be equal to 200 ms, which equals five time steps of acquisitions. This is much smaller than the mean duration of a chaotic transient, and even smaller than the characteristic time of the system (around one or two seconds). Taking all acquisitions into account, one defines the mean defect rate

$$\langle \rho \rangle = \frac{1}{N} \sum \rho_k, \tag{5}$$

where ρ_k is the defect-rate related to the kth acquisition and N_{acq} the number of acquisitions ($N_{\mathrm{acq}}=250$).

Figures 13(a)–13(f) are plots of the mean defect-rate versus time, for different flow rates. They are worth some comments.

To enable the fit procedure to run correctly, it is necessary to add an arbitrary (but negligible in regards to the experimental noise) value of 10^{-8} s^{-1} to the mean defect rate, so that the fit procedure proceeds until the time corresponding to the occurrence of the last reported defect.

The time from which data are fitted should not be smaller than the characteristic time of the pattern: that is the reason why these plots start from $t=1$s. Between the first second (from $t=0$ to $t=1$ s), sequences of abnormally high defect rates are not taken into account.

Plots (b) – (f) are correctly fitted by a power law, with an exponent α which tends to increase approaching Γ_c:

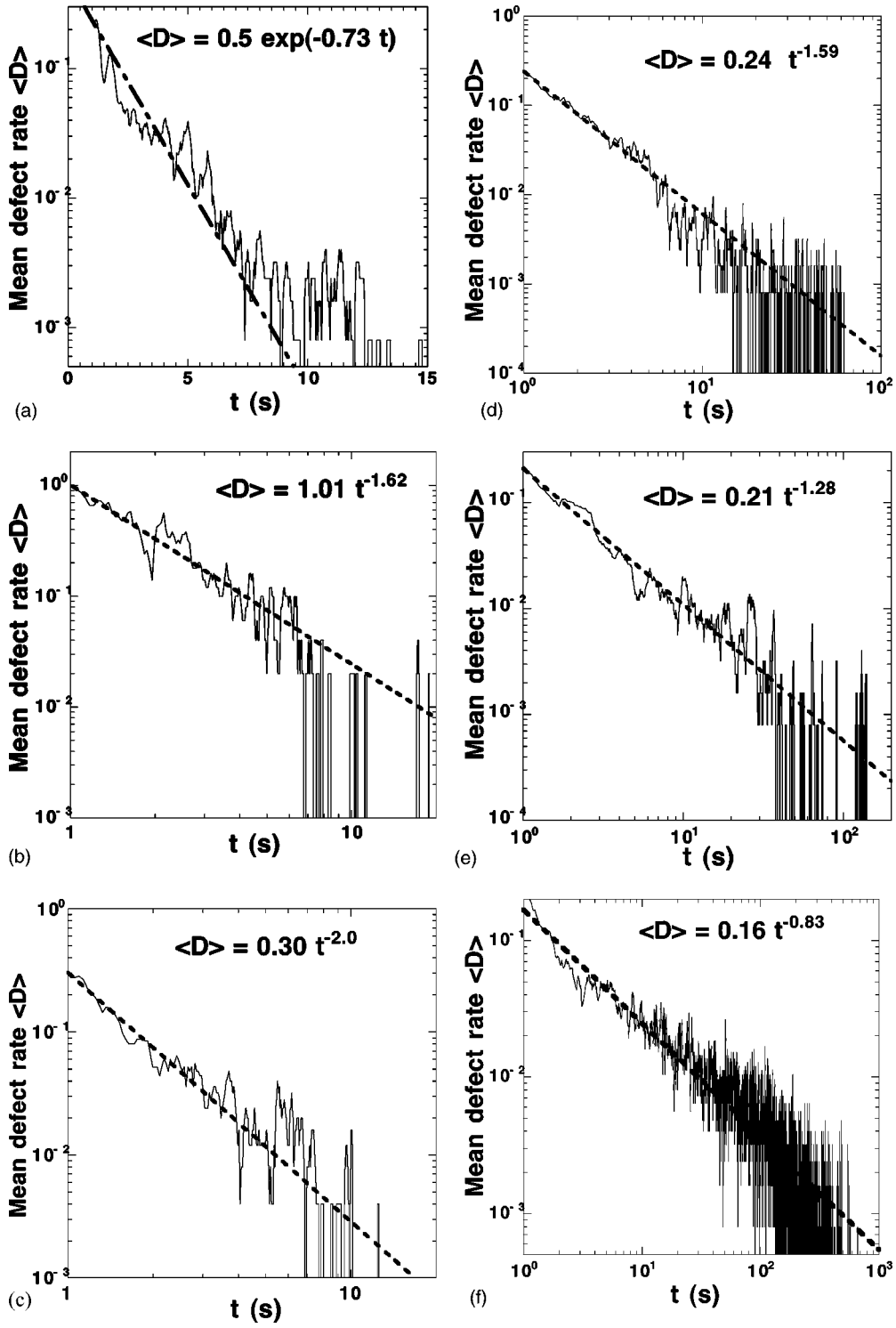

FIG. 13. Mean defect rate versus time during chaotic transients. (a) – (f) are plots at increasing flow rates (Γ equals successively 0.136, 0.232, 0.245, 0.277, 0.300, and 0.315 cm^2/s). The dotted lines stands for the median value of the best fit.

$$\langle \rho \rangle \sim t^{-\alpha_{\mathrm{eff}}(\Gamma)}, \tag{6}$$

where α_{eff} is an effective exponent, dependent upon flow rate, which extrapolated value on threshold equals α. Figure 14 shows the measured effective exponents versus flow rate. An empirical curve is built (dotted line), and according to the variation range found for Γ_c [see Eq. (3)], one can extract by extrapolation to threshold, a range of values for the critical exponent α:

$$\alpha = -0.6 \pm 0.15. \tag{7}$$

The values for γ and α are different than those obtained in directed percolation. Nevertheless, it is not the main point of

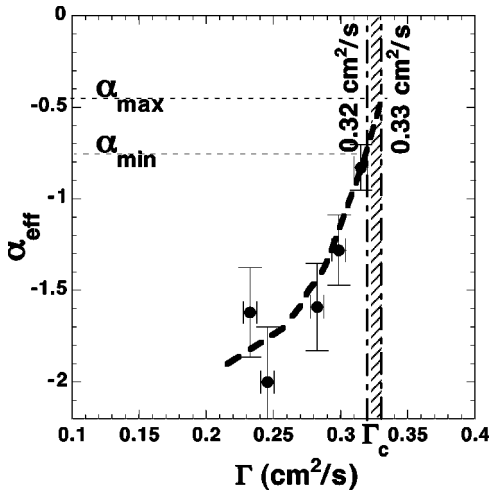

FIG. 14. Effective exponent providing the best algebraic fit of density decrease versus time [see Figs. 13(b)–13(f)].

interest of our study. In the search for critical phenomena, the measurement of these exponents should instead emphasize that the defect rate is a natural and convincing measure of disorder, and that chaotic transients can be interesting to study as well as permanent states, provided that a sufficiently large number of acquisitions are run. This condition is not necessary when chaos is permanent, which is presented in the next section.

V. STATISTICAL STUDIES OF CHAOTIC STATES

If $\Gamma > \Gamma_c$, the pattern endlessly exhibits defects and chaotic dynamics. The study of chaotic states is simpler than transients, because it is not necessary to run the system from many different initial conditions. Sufficiently long acquisitions are supposed to capture most of the statistical features which are of interest here.

After a long wait (typically 30 min), an acquisition is started. Its duration is approximately twenty minutes (30 000 time steps). Defects are counted during acquisitions and the defect rate is deduced, still defined as in Eq. (4). It is generally found (at least far from threshold) that the defect rate does not fluctuate during a complete acquisition, the cumulative number of defects appears as a quite straight line versus time. This means that the defect rate should not depend on the parameter δt, the time interval during which the defect sum is calculated, provided that δt is larger than ten time steps (400 ms). However, this is no longer true for acquisitions close to threshold. Indeed, just above Γ_c, long laminar phases can be observed alternatively amongst chaotic phases. An example of such behavior, frequently observed just above threshold, is illustrated on Figs. 15(a) and 15(b). When the flow rate is increased, the duration of these laminar phases rapidly decreases. The typical flow rate above which these phases are of same order of magnitude as the characteristic time of the system, or shorter, is around 0.39 cm^2/s (then a relative distance to threshold around 20%). It is thus necessary to keep in mind this behavior before the presentation of measurements of disorder during chaotic states.

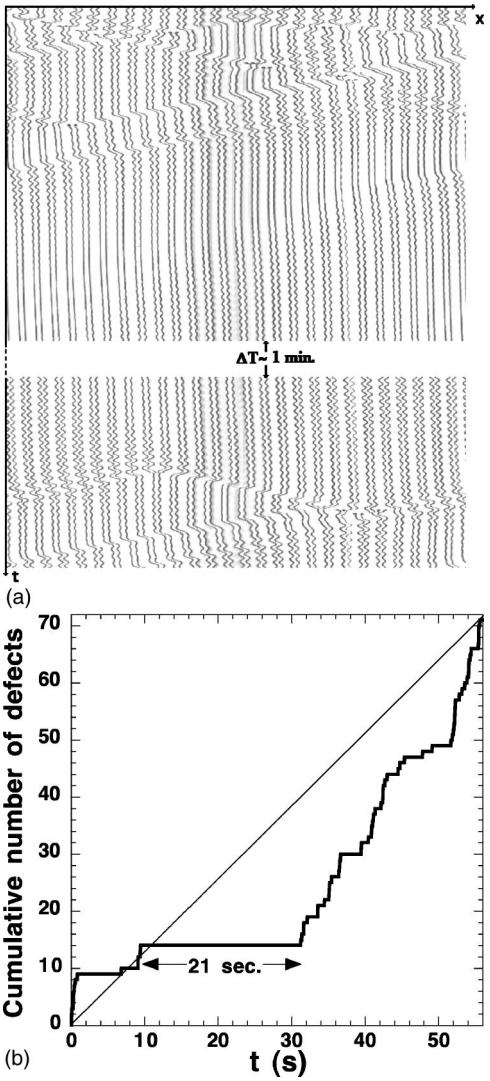

FIG. 15. (a) Existence of long laminar (defect-free) phases, just above threshold ($\Gamma = 0.343$ cm^2/s). (b) Defect-rate versus time, at the same flow rate than (a) but for another acquisition, showing a significant defect-free phase of duration around 21 s. The slope of the line stands for the mean defect rate during this extract.

In order to measure the disorder dependance with the distance to threshold, several long acquisitions are done: two or three runs per flow-rate value, except near threshold where 5 to 12 acquisitions per flow-rate values are done (mainly for the dish of radius 5 cm). Results are plotted in Figs. 16(a) and 16(b). Figure 16(b) is a magnified plot of (a) near threshold. Each point represents a mean defect rate during an acquisition of 30 000 time steps. These plots reveal several facts. The mean defect rate increases, with a seemingly linear law, with the flow-rate difference $(\Gamma - \Gamma_c)$. The defect rate is larger with a dish of larger radius. The ratio of two defect rates, for the two different dish and the same flow rate, does not equal the ratio of dish radius. Close to threshold, measurements are more dispersed [see Fig. 16(b)]. This is due to the occurrence of the long laminar phases introduced above. Then, a duration of twenty minutes is not long enough to measure a consistent mean value. That is the reason why the mean defect rate has to be deduced from several consecutive

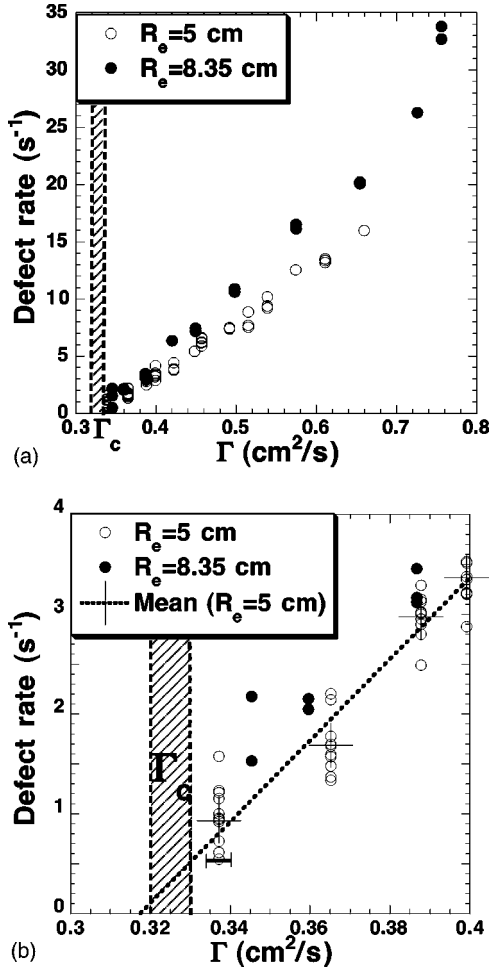

FIG. 16. (a) Mean defect rate during acquisitions of duration twenty minutes, showing a quite linear increase with flow rate, for two dish radius. (b) Zoom of (a) in the threshold vicinity, showing a significant dispersion of data, due to long laminar phases. Crosses represent the mean under several acquisitions (radius R_e=5 cm), and the hatched area is the range for Γ_c.

acquisitions, as some memory limitations in our computer do not allow acquisitions longer than 20 min. The large crosses in Fig. 16(b) stand for mean defect-rate values; the dotted line is a linear fit deduced from these values. Sufficiently far from threshold, the deviation from an acquisition to another is small.

From these data, the defect-rate appears as a seemingly power law versus the distance to threshold

$$\langle \rho \rangle \sim (\Gamma - \Gamma_c)^{\beta}. \tag{8}$$

The question is now which range of data has to be taken into account for the determination of β, knowing that Eq. (8) is supposed to be reliable only near threshold? Moreover, it is worth to mention that, as soon as the defect rate overcomes 10 to 15 defects per second, the counting is limited by possibly non-negligible occurrences of simultaneous creation and disappearance of columns during the same time step [''(+1)(−1)'' events mentioned above]. This could lead to an underestimated defect rate far from threshold. Thus, measurements far from threshold have finally not been taken into account for the determination of the critical exponent β; the limit of validity has been chosen from 0.33 to 0.55 cm^2/s.

The value for β is found equal to

$$\beta = 1.0 \pm 0.1. \tag{9}$$

In most experimental systems exhibiting STI, β is deduced from the "turbulent" fraction (the relative chaotic surface in spatiotemporal diagrams) versus the relative distance to threshold. A question would then essentially need to be answered: could the defect rate be measured in others systems, and in such a case, would it provide results comparable to the values obtained with the turbulent fractions? Studies of some systems seemingly involving defects, such as directional solidification, printer's instability, or ferrofluid pikes, could possibly answer this question. Another possible further way of investigations would be to determine the distribution of durations of defect-free phases. Such calculus has been tried but because of the cutoff due to the finite time step (1/25 s) during acquisitions, the obtained data cover barely more than one decade in time and are not conclusive. After quantitative studies of critical properties, in a framework comparable to that used in STI, it is now of interest to return to specific points which enlighten how the pattern of columns is different than systems involving STI.

VI. BACK TO MECHANISMS INVOLVED IN DISORDER

This section presents a qualitative overview of mechanisms involved in disorder and shows why chaos in our system is different than chaos via STI occurring in most of the systems mentioned above. In several pattern-forming instabilities (such as the Rayleigh-Bénard convection, the Taylor-Couette system, etc.), transition to chaos occurs via STI, which appears as turbulent patches, comparable to the spots observed in the plane Couette flow. Within a chaotic regime, the pattern is no longer constituted by identical cells: in turbulent domains, the shape of the cells fluctuates (see, for example, Fig. 4 of Ref. [8]). Chaos appears in a different way in the array of columns, in the sense that the morphology of the cells is the same in both predictable and chaotic regimes. This means that the pattern of columns cannot be divided between laminar and turbulent patches, as already noted. This also signifies that the features which constitutes disorder do not lie in the morphology of cells, but rather depends on their relative motions. This last sentence suggests that basic dynamical regimes get involved in disorder, although they constitute completely laminar and predictable states when they are isolated.

Particularly sound is the role of propagative domains. They have been previously studied through their intrinsic properties in nonchaotic regimes [17,19], which are presumably linked to mechanisms creating and sustaining disorder. In the following, we give a short summary of these features.

The wavelength inside a domain can adjust itself in a broad range of values (around 30% of the median value), but the wavelength outside is selected at a fixed value λ_0 independent on flow-rate and others geometrical parameters.

For sufficiently high flow-rates, the wake following a domain at the selected wavelength λ_0 involves oscillating col-

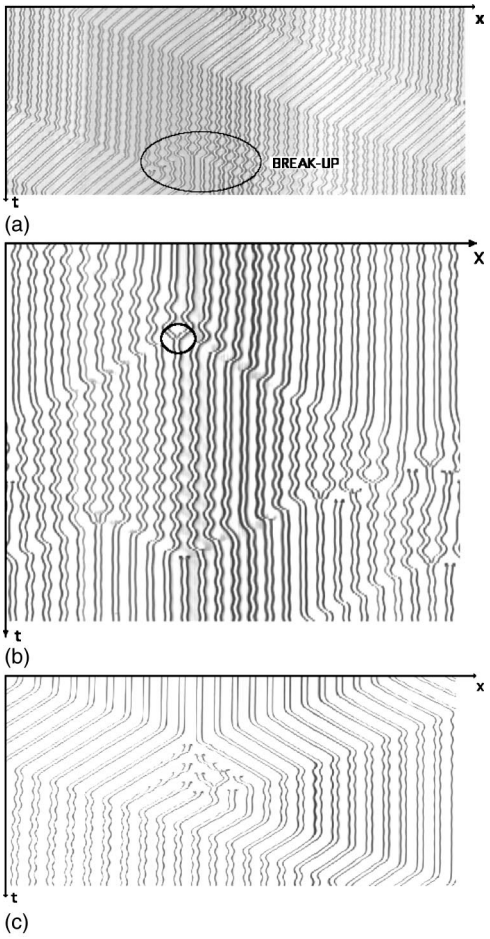

FIG. 17. Illustrations of mechanisms creating disorder. (a) An oscillatory wake created behind a propagative domain can destabilize and make the pattern entering the STC regime. (b) A defect launches two small propagative domains, that are going to collide and create new defects. (c) Two colliding propagative domains generate defects.

umns. These oscillations can amplify and lead to defects [see Fig. 17(a)].

When two domains propagate to the same direction, the velocity of their walls become equal after a very short time, so that they never encounter. When two domains propagate to opposite directions, they collide and generate defects [see Fig. 17(c)]. The final state is a propagative domain, the size of which is a subtraction of the sizes of initial domains (or a static state if the initial sizes were equal). Moreover, the link between colliding domains and defect creations is bilateral: defects can launch propagative domains that meet and create other new defects [Fig. 17(b)]. This constitutes the main part of disorder sustaining. The same kind of behavior can be produced by CML, and it has been shown that if such colliding solitary structures are sources of disorder, they can play a role in the universality class of the system [27].

Although drifting columns appear in localized structures, it has been shown that the corresponding bifurcation is supercritical. More generally, secondary bifurcations are continuous in the array of columns [18]. Observation of STI in such a system is possible only if at least one of the successive bifurcations is subcritical. So that this definitely dismiss the transition scenario via STI.

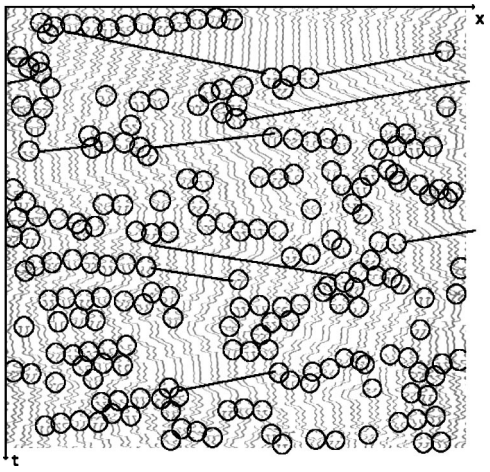

FIG. 18. Diagram evidencing the coupled roles of defects and propagative structures in disorder sustaining.

However, it does not mean that a contamination process does not exist in this system, especially because propagative structures can spread disorder in a specific way. We illustrate more clearly these complex mechanisms in an example of globally disordered pattern: Fig. 18 presents a spatiotemporal diagram in which we have drawn black circles around each defect (as a zone of influence) [37]. On the same diagram, some edge walls of propagative domains are represented by black lines.

This diagram shows that defects can appear isolated, or within small groups, and do not seem to spread by contamination, contrary to what is observed in turbulent domains of STI. However, these groups of defects seem to be connected with each other by propagative domains, as is suggested by several straight lines. Thus disorder, although involving unpredictable dynamics, is constituted by deterministic blocks (propagative domains or oscillating patches). This is not paradoxical, if one considers that the loss of spatial or temporal symmetries are generally first steps toward complex phenomena. What seems to be original in the pattern of columns, is that these deterministic blocks give rise to defects, which seem to constitute the real cause of unpredictability, as in the CGLE equation, for example. A similar scenario could occur in related systems, such as fluid fronts or in some patterns obtained in directional solidification [1,14,15] where, to our knowledge, no quantitative study of chaotic regimes has been done until now.

VII. CONCLUSION

To conclude, we have presented a quantitative study of disordered states in the pattern of falling liquid columns. Disorder in our system does not appear as the coexistence of laminar and turbulent domains, and thus is not included in the usual definition of spatiotemporal intermittence. By adapting the usual framework of STI to the specific properties of our system, we have measured three critical exponents, with satisfactory ranges of error despite finite-size ef-

fects. Thus, it has been shown that occurrences of defects, which cause unpredictable dynamics, can quantify disorder in such a pattern. The defect rate then appears as a natural measure of disorder, such as the usual "turbulent fraction" in STI. It should be of interest to apply this framework to patterns with destabilizing interfaces, where dynamical behaviors are similar.

Another original framework, used here to determine critical properties, is to approach the threshold from minor values, where chaotic dynamics are transient. In particular, it has been demonstrated that a statistical study of chaotic transients can lead to measure the divergence of a characteristic duration. A similar quantity is usually measured approaching the threshold from above, deduced from time distributions or by mean durations of laminar domains lying in STI regimes [8–10,12,21,22].

This study also emphasizes the role of propagative structures in the creation of disorder: first, they give rise to an oscillating wake that can amplify and break; second, their multiple collisions generate defects. Reciprocally, defects themselves create small propagative domains that are going to collide and loop the contaminative process. This suggests that disorder appears in our system as an ensemble of deterministic blocks (propagative domains or oscillations), strongly interacting with each others. That is also the reason why disorder is never localized. Disorder then appears globally, even just above threshold, and is perhaps the most essential difference with systems exhibiting a transition via STI. Then, the nature of this chaos could be related to "defect mediated turbulence," even if there is no definitive proof.

Let us finally mention the recent observations of a two-dimensional extension of this experiment [44,45]: in a 2D pattern of columns, disorder seems to be able to localize into domains coexisting with static ones. Between order and disorder, a separative front can stay stable for a long time, which constitutes a major difference from the 1D array. Dynamical regimes not observed in the 1D array have been reported in Ref. [44], where a flow state diagram is also presented.

ACKNOWLEDGMENTS

We are indebted to H. Chaté for many relevant suggestions. We would also like to thank J.-M. Flesselles, S. Bottin, and M. van Hecke for fruitful discussions.

[1] J. M. Flesselles, A. J. Simon, and A. J. Libschaber, Adv. Phys. **40**, 1 (1991).
[2] M. C. Cross and P. C. Hohenberg, Rev. Mod. Phys. **65** 851 (1993).
[3] P. Coullet and G. Iooss, Phys. Rev. Lett. **64** 866 (1990).
[4] P. Manneville, *Dissipative Structures and Weak Turbulence* (Academic, New York, 1990).
[5] T. Bohr, M. H. Jensen, G. Paladin, and A. Vulpiani, *Dynamical Systems Approach to Turbulence* (Cambridge University Press, Cambridge, 1998).
[6] C. Normand, Y. Pomeau, and M. G. Velarde, Rev. Mod. Phys. **49**, 581 (1977).
[7] S. Ciliberto and P. Bigazzi, Phys. Rev. Lett. **60**, 286 (1988).
[8] F. Daviaud, M. Bonetti, and M. Dubois, Phys. Rev. A **42** 3388 (1990).
[9] M. M. Degen, I. Mutabazi, and C. D. Andereck, Phys. Rev. E **53**, 3495 (1996).
[10] P. W. Colovas and C. D. Andereck, Phys. Rev. E **55**, 2736 (1997).
[11] M. Rabaud, S. Michalland, and Y. Couder, Phys. Rev. Lett. **64** 184 (1990).
[12] S. Michalland, M. Rabaud, and Y. Couder, Europhys. Lett. **22** 17 (1993).
[13] L. Pan and J. R. de Bruyn, Phys. Rev. E **49**, 483 (1994).
[14] A. J. Simon, J. Bechhoefer, and A. Libchaber, Phys. Rev. Lett. **61**, 2574 (1988).
[15] M. Ginibre, S. Akamatsu, and G. Faivre, Phys. Rev. E **56** 780 (1997).
[16] C. Counillon, L. Daudet, T. Podgorski, and L. Limat, Phys. Rev. Lett. **80**, 2117 (1998).
[17] P. Brunet, J.-M. Flesselles, and L. Limat, Europhys. Lett. **56**, 221 (2001).
[18] P. Brunet Ph.D. thesis, Paris VI University, 2002.
[19] P. Brunet, J.-M. Flesselles, and L. Limat, Eur. Phys. J. B **35**, 525 (2003).
[20] F Melo and S. Douady, Phys. Rev. Lett. **71**, 3283 (1993).
[21] D. P. Vallette, G. Jacobs, and J. P. Gollub Phys. Rev. E **55**, 4274 (1997).
[22] P. Rupp, R. Richter, and I. Rehberg, Phys. Rev. E **67**, 036209 (2003).
[23] M. I. Rabinovich, A. B. Ezersky, and P. D. Weidman, *The Dynamics of Patterns* (World Scientific Publishing, Singapore, 1998).
[24] P. Bergé, Y. Pomeau, and C. Vidal, *L'espace Chaotique* (Hermann Editions, Paris, 1998).
[25] Y. Pomeau, Physica D **23**, 3 (1986).
[26] H. Chaté and P. Manneville, Phys. Rev. Lett. **58** 112 (1987); H. Chaté and P. Manneville, Physica D **32**, 409 (1988).
[27] G. Rousseau, Ph.D. thesis, Paris VII University, 1998.
[28] T. Bohr, M. van Hecke, R. Mikkelsen, and M. Ipsen, Phys. Rev. Lett. **86**, 5482 (2001).
[29] R. Mikkelsen, M. van Hecke and T. Bohr, Phys. Rev. E **67**, 046207 (2003).
[30] S. Bottin and H. Chaté, Eur. Phys. J. B **6**, 143 (1998).
[31] This remark prefigures a debate about what one considers as laminar domains. An answer, which works for our system at least, is given in Sec. III.
[32] The number of cells rarely exceed a hundred, since simulations of CML were done with several hundreds of sites.
[33] Y. Kuramoto, *Chemical oscillations, Waves and Turbulence* (Springer-Verlag, Berlin, 1978).
[34] G. I. Sivashinsky, Acta Astronaut. **4**, 1177 (1977).
[35] C. Misbah and A. Valance, Phys. Rev. E **49**, 166 (1994).
[36] K. R. Elder, J. D. Gunton, and N. Goldenfeld, Phys. Rev. E

56, 1631 (1997).
[37] H. Chaté (private communication).
[38] P. Coullet, L. Gil, and J. Lega, Phys. Rev. Lett. **62**, 1619 (1989).
[39] I. Rehberg, S. Rasenat, and V. Steinberg, Phys. Rev. Lett. **62** 756 (1989).
[40] I. Aranson, H. Levine, and L. Tsimring, Phys. Rev. Lett. **76**, 1170 (1996).
[41] K. E. Daniels and E. Bodenschatz, Phys. Rev. Lett. **88**, 034501 (2002).
[42] D. A. Egolf, I. V. Melnikov, W. P. Pesch, and R. E. Ecke, Nature (London) **404**, 733 (2000).
[43] M. Howard and M. van Hecke, Phys. Rev. E **68**, 026213 (2003).
[44] C. Pirat, C. Mathis, P. Maissa, and L. Gil, Phys. Rev. Lett. **92**, 104501 (2004).
[45] P. Brunet, G. Gauthier, L. Limat, and D. Vallet, Exp. Fluids (to be published).